NAVAL POSTGRADUATE SCHOOL

MONTEREY, CALIFORNIA

THESIS

EFFECTS OF CARBON NANOMATERIAL REINFORCEMENT ON COMPOSITE JOINTS UNDER CYCLIC AND IMPACT LOADING

by

Meng Hwee Tan

March 2012

Thesis Advisor:	Young W. Kwon
Second Reader:	Randall D. Pollak

Approved for public release; distribution is unlimited

THIS PAGE INTENTIONALLY LEFT BLANK

REPORT DOCUMENTATION PAGE			Form Approved OMB No. 0704-0188
Public reporting burden for this collection of information is estimated to average 1 hour per response, including the time for reviewing instruction, searching existing data sources, gathering and maintaining the data needed, and completing and reviewing the collection of information. Send comments regarding this burden estimate or any other aspect of this collection of information, including suggestions for reducing this burden, to Washington headquarters Services, Directorate for Information Operations and Reports, 1215 Jefferson Davis Highway, Suite 1204, Arlington, VA 22202-4302, and to the Office of Management and Budget, Paperwork Reduction Project (0704-0188) Washington DC 20503.			
1. AGENCY USE ONLY *(Leave blank)*	**2. REPORT DATE** March 2012	**3. REPORT TYPE AND DATES COVERED** Master's Thesis	
4. TITLE AND SUBTITLE Effects of Carbon Nanomaterial Reinforcement on Composite Joints Under Cyclic and Impact Loading		**5. FUNDING NUMBERS**	
6. AUTHOR(S) Meng Hwee Tan			
7. PERFORMING ORGANIZATION NAME(S) AND ADDRESS(ES) Naval Postgraduate School Monterey, CA 93943-5000		**8. PERFORMING ORGANIZATION REPORT NUMBER**	
9. SPONSORING /MONITORING AGENCY NAME(S) AND ADDRESS(ES) N/A		**10. SPONSORING/MONITORING AGENCY REPORT NUMBER**	
11. SUPPLEMENTARY NOTES The views expressed in this thesis are those of the author and do not reflect the official policy or position of the Department of Defense or the U.S. Government. IRB Protocol number _____N/A_____.			
12a. DISTRIBUTION / AVAILABILITY STATEMENT Approved for public release; distribution is unlimited		**12b. DISTRIBUTION CODE** A	

13. ABSTRACT (maximum 200 words)

This study investigated the influence of Multi-Walled Carbon Nanotubes (MWCNTs) and Carbon Nanofibers (CNFs) reinforcement on the behavior of Carbon Fiber Reinforced Polymer (CFRP) joint interface under cyclic and impact loading. Test coupons with pre-cracks were fabricated via Vacuum Assisted Resin Transfer Molding (VARTM) technique with 7.5g/m2 of MWCNTs or CNFs dispersed at the joint interface ahead of the crack tip. The test coupons were loaded in 3-point bending at 2Hz and 10Hz frequencies for the cyclic loading test. The CNTs and CNFs-reinforced samples displayed higher stiffness and had significantly shorter crack propagation lengths under the same loading cycles. Resistance to crack propagation was evident in the reinforced samples as observed using an optical microscope. Similar sets of reinforced as well as non-reinforced samples were subjected to low energy impact tests and their dynamic responses and failures were also compared. CNTs-reinforcement samples experienced failure at higher impact force as compared to non-reinforced samples. However, further testing was recommended to establish the effects of CNFs reinforcement under impact loading. The test results suggested that proper reinforcement of the joint interface using carbon nanomaterial can significantly delay the crack growth, resulting in improvement of composite structural integrity and its service life.

14. SUBJECT TERMS Carbon nanotubes, carbon nanofibers, composite joints, , cyclic loading, impact loading			**15. NUMBER OF PAGES** 65
			16. PRICE CODE
17. SECURITY CLASSIFICATION OF REPORT Unclassified	**18. SECURITY CLASSIFICATION OF THIS PAGE** Unclassified	**19. SECURITY CLASSIFICATION OF ABSTRACT** Unclassified	**20. LIMITATION OF ABSTRACT** UU

NSN 7540-01-280-5500

Standard Form 298 (Rev. 2-89)
Prescribed by ANSI Std. 239-18

THIS PAGE INTENTIONALLY LEFT BLANK

Approved for public release; distribution is unlimited

EFFECTS OF CARBON NANOMATERIAL REINFORCEMENT ON COMPOSITE JOINTS UNDER CYCLIC AND IMPACT LOADING

Meng Hwee Tan
ME5, Singapore Navy
B.S., Nanyang Technological University, 2002

Submitted in partial fulfillment of the
requirements for the degree of

MASTER OF SCIENCE IN MECHANICAL ENGINEERING

from the

NAVAL POSTGRADUATE SCHOOL
March 2012

Author: Meng Hwee Tan

Approved by: Young W. Kwon
Thesis Advisor

Randall D. Pollak
Second Reader

Knox T. Millsaps
Chair, Department of Mechanical and Aerospace Engineering

THIS PAGE INTENTIONALLY LEFT BLANK

ABSTRACT

This study investigated the influence of Multi-Walled Carbon Nanotubes (MWCNTs) and Carbon Nanofibers (CNFs) reinforcement on the behavior of Carbon Fiber Reinforced Polymer (CFRP) joint interface under cyclic and impact loading. Test coupons with pre-cracks were fabricated via Vacuum Assisted Resin Transfer Molding (VARTM) technique with 7.5g/m^2 of MWCNTs or CNFs dispersed at the joint interface ahead of the crack tip. The test coupons were loaded in 3-point bending at 2Hz and 10Hz frequencies for the cyclic loading test. The CNTs and CNFs-reinforced samples displayed higher stiffness and had significantly shorter crack propagation lengths under the same loading cycles. Resistance to crack propagation was evident in the reinforced samples as observed using an optical microscope. Similar sets of reinforced as well as non-reinforced samples were subjected to low energy impact tests and their dynamic responses and failures were also compared. CNTs-reinforcement samples experienced failure at higher impact force as compared to non-reinforced samples. However, further testing was recommended to establish the effects of CNFs reinforcement under impact loading. The test results suggested that proper reinforcement of the joint interface using carbon nanomaterial can significantly delay the crack growth, resulting in improvement of composite structural integrity and its service life.

THIS PAGE INTENTIONALLY LEFT BLANK

TABLE OF CONTENTS

THIS PAGE INTENTIONALLY LEFT BLANK

LIST OF FIGURES

LIST OF TABLES

THIS PAGE INTENTIONALLY LEFT BLANK

LIST OF ACRONYMS AND ABBREVIATIONS

CFRP	Carbon Fiber Reinforced Polymer
CNFs	Carbon Nanofibers
CNTs	Carbon Nanotubes
CoNap	Cobalt Naphthenate
DMA	N-Dimethylaniline
LCS	Littoral Combat Ship
MEKP	Methyl Ethyl Ketone Peroxide
MWCNT	Multi-Walled Carbon Nanotube
USV	Unmanned Surface Vehicle
VARTM	Vacuum-Assisted Resin Transfer Molding

THIS PAGE INTENTIONALLY LEFT BLANK

ACKNOWLEDGMENTS

I would like to express my heartfelt appreciation to the following people who have given their support toward the completion of this thesis study.

My thesis advisor, Professor Young W. Kwon, for his patience and guidance for the past one year. Without his vast knowledge and expertise in this field of research, this thesis would not be as complete.

Professor Claudia C. Luhrs, for the provision of carbon nanofibers used in the research.

Dr. Chanman Park, for his assistance on the operation of the MTS machine and microscope.

Thomas Christian, for his assistance on the operation of the impact machine and setting of strain gauges on the specimens.

Integrated Composite, particularly Mr. Rey Uncangco, for the use of their water-jet cutting machine during the course of my research.

Special thanks to the Republic of Singapore Navy for giving me the opportunity to widen my knowledge at Naval Postgraduate School (NPS).

My wife, Chiu Teng Lim, for her understanding and support throughout my study at NPS and not forgetting her delicious meals and bakes.

Last, but not least, I would like to thank Nami (our pretty Shih Tzu) for keeping my wife company when I was busy in school.

THIS PAGE INTENTIONALLY LEFT BLANK

I. INTRODUCTION

A. BACKGROUND

1. Composite Materials

Combining two or more different materials creates a third, new material, commonly known as a composite. Composites have improved properties different from the original materials. In most cases, one material serves as the matrix while the other acts as reinforcement.

The use of composite materials goes a long way back to when straw was used to strengthen mud brick. In more recent contexts, fibrous material is used to reinforce resin matrix. Fibers inherently are much stiffer and stronger than their bulk suggests, and they have high strength-to-density ratios and high stiffness-to-density ratios. Carbon fiber has a high tensile strength of 1.7 GPa and tensile stiffness of 190 GPa [1], making carbon fiber reinforced polymer (CFRP) a popular choice for its strength and light weight. In this study, plain weave carbon fiber fabric was used to reinforce vinyl ester resin matrix.

2. Naval Applications

While composite materials have been used significantly for aircraft structures, they are being used more and more in naval applications. For example, the superstructure of DDG1000 is made of carbon composites. Littoral Combat Ship (LCS) is being considered to be constructed by composite materials. Nanomaterial supplier Zyvex Performance Materials [2] unveiled an unmanned surface vehicle (USV) constructed from nanotube-reinforced carbon fiber prepreg.

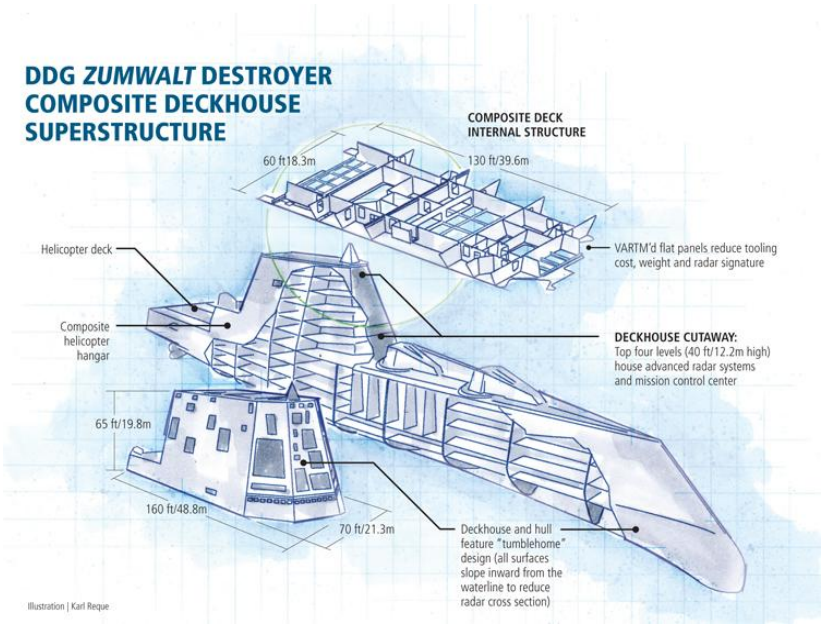

Figure 1. Composite decks on DDG1000. (From [3])

Figure 2. USV built from nanotube-reinforced carbon fiber composites. (From [2])

Composite structures are light but stiff and strong. As a result, there is a significant saving in costs in terms of operating the composite ship because the fuel consumption is much lower than conventional steel ships. Besides, corrosion resistance of composite materials makes them ideal for marine environments, driving down the maintenance costs.

Large structures such as ships cannot be constructed as a single piece due to practicability. As a result, it is necessary to join multiple pieces together. For conventional metals, welding has been used for joining. For composite structures, welding is not applicable. Instead, scarf joints have been used. The joint section is generally the weakest link of the structure.

3. Carbon Nanomaterial

Nanotechnology is one of the most important technology advancements in this century, driving material science research to new heights. Carbon nanotubes (CNTs) are allotropes of carbon with a cylindrical nanostructure. CNTs are the strongest and stiffest materials discovered in terms of tensile strength and elastic modulus, respectively. Coupled with light weight, CNTs are ideal for carbon fiber composite reinforcement. The main disadvantage, however, is the high cost of production for commercial applications despite the strides in nanotechnology. A possible alternative for composites additives is carbon nanofibers (CNFs). CNFs are not as strong compared to CNTs but production costs are lower.

The difficulty in dispersing CNTs uniformly in the resin matrix decreased the performance benefits of the nanomaterial reinforcement. Some techniques had been applied to disperse the CNTs more uniformly such as functionalization of the CNTs [4]. However, researches are still working to achieve an optimum distribution of CNTs.

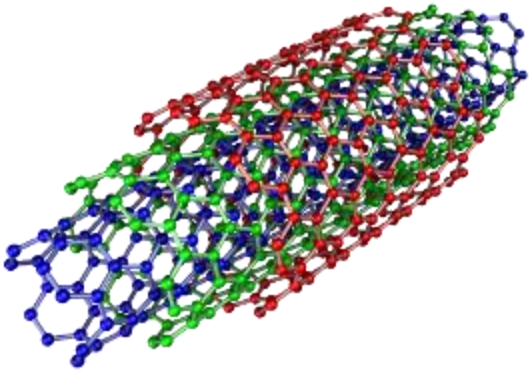

Figure 3. Multi-walled CNTs

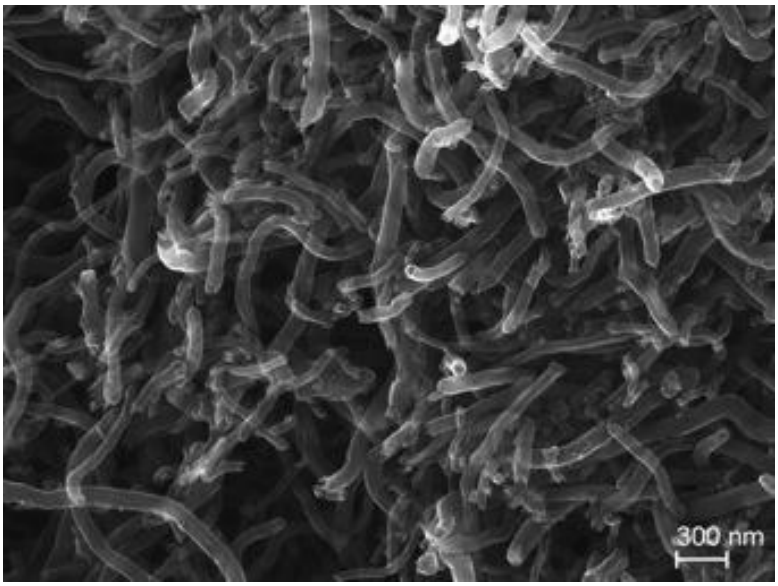

Figure 4. CNFs under scanning electron microscope (From Professor Claudia C. Luhrs, Naval Postgraduate School, 2011)

B. LITERATURE REVIEW

Numerous studies had been carried out to investigate the effects of CNTs reinforcement on CFRP. It had been proven that the infusion of CNTs enhances the strength and fracture toughness of CFRP laminates under static loading (mode I and mode II). Kostopoulos et al. [5] investigated the influence of the multi-walled carbon nanotubes (MWCNTs) on the impact and after-impact behavior of CFRP laminates. Enhanced performance was observed for the CNTs reinforcement specimens for higher energy impact and after–impact fatigue life. Literatures [6]–[8] focused on the investigation of using CNTs network to sense and distinguish different types of damage under impact and cyclic loadings.

Besides the impracticability of manufacturing composite in one large complete piece, it is also very costly to infuse CNTs throughout the laminates. There were studies focusing on effects of CNTs reinforcement on composite adhesive joints. Faulkner and Kwon [9] observed improvement in strength and fracture toughness of CFRP joints with CNTs reinforcement under Mode I and Mode II testing. Burkholder et al. [4] showed that multi-walled CNTs (MWCNTs) reinforcement could improve fracture toughness of steel-composite and composite-composite adhesive joints under Mode II testing. These studies focused at the enhancement under static loading. It is therefore necessary to extend the studies to investigate the effects of CNTs reinforcement on composite joints under cyclic and impact loading.

C. OBJECTIVES

The aim of this research study is to investigate the influence of CNTs and CNFs reinforcement on CFRP joint interface under cyclic and impact loading. The specimens were loaded in 3-point bending at 2Hz and 10Hz frequencies for the cyclic loading test. Similar sets of reinforced as well as non-reinforced samples were subjected to low energy impact tests and their dynamic responses and failures were also compared. The objective was to determine if the reinforcement improved the properties of the CFRP and thus improving structural integrity and service life. Another objective was to explore the possibility of using CNFs as a cheaper alternative to CNTs reinforcement.

THIS PAGE INTENTIONALLY LEFT BLANK

II. CONSTRUCTION OF COMPOSITE SAMPLE

A. MATERIALS

CFRP test samples were constructed using Toray T700 CF carbon fiber plain weave fabrics with Derakane 510A epoxy vinyl ester resin. The desired curing time based on manufacturer's recommendation for Derakane 510A is 60 minutes. Methyl Ethyl Ketone Peroxide (MEKP) and Cobalt Naphthenate (CoNap) were the hardening chemicals used in the fabrication process. MEKP was used to initiate the curing process while CoNap acted as the accelerator determining the curing time. A third chemical, N-Dimethylaniline (DMA) was required for ambient temperatures below 70^{o}F to ensure a curing time of less than 60 minutes. All three chemicals added were to assist in the curing process and had no effect on the properties of the final composite sample. Table 1 listed the required percentage of the respective chemicals at different ambient temperatures.

Table 1. Proportions of hardening chemicals

Temperature	Chemicals	Proportions
15-20^{o}C	MEKP	1.25%
Cool 60s^{o}F	Cobalt	0.30%
	DMA	0.05%
21-26^{o}C	MEKP	1.00%
Mid 70^{o}F	Cobalt	0.20%
	DMA	-

MWCNTs (outer diameter 30±15nm, length 5–20 micron, purity > 95%) were used for the composite joint interface reinforcement. Kwon et al. [10] investigated on the method of dispersion and surface concentration of CNTs. A 7.5g/m^2 surface concentration with acetone dispersion was found to optimize the effect of CNTs reinforcement on the joint interface. The CNFs used in the research were fabricated in-house at the Mechanical and Aerospace Department, Naval Postgraduate School. The nominal diameter was 100nm.

B. TEST COUPON SPECIFICATIONS

1. Cyclic Loading

Four sample sets were constructed to investigate the effect of CNTs and CNFs reinforcement on crack propagation under cyclic loading. The first set consists of non-reinforced coupons. The other three sets were fabricated with CNTs, CNFs and mixed CNTs/CNFs reinforcement at the joint interface, respectively. The samples were cut, using water-jet cutting machine, into coupons as shown in Figure 5.

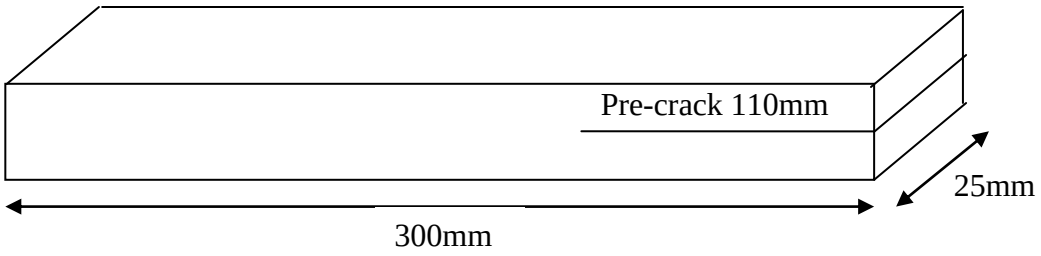

Figure 5. Coupon dimensions for cyclic loading

2. Impact Testing

For the impact loading, three sets were fabricated with two sets being reinforced with CNTs and CNFs, respectively, and one without any reinforcement at the joint interface. The samples were cut into test coupons with dimensions indicated in Figure 5.

C. FABRICATION PROCEDURES

1. Vacuum-Assisted Resin Transfer Molding

Vacuum-Assisted Resin Transfer Molding (VARTM) is a common technique used in the industry for the construction of composite materials. VARTM utilizes the process of vacuum infusion to evenly distribute the liquid resin throughout the carbon fiber fabric. VARTM is a cost effective and fast method of constructing composite structure. VARTM also does not affect the dispersion of the carbon nanomaterial on the joint interface during the infusion process.

Figure 6 showed the setup of VARTM in the laboratory. The vacuum created via the vacuum pump would draw the liquid resin, from the reservoir, through the layers of carbon fabrics. The excess resin was drained into the resin trap. The composite laminate was left to cure and harden for 20 hours prior to removal.

Figure 6. VARTM setup in the laboratory

2. Two-Step Curing

The test coupons with the pre-crack length for both testing were constructed using two-step curing process. Bily [11] determined that composite joint interfaces constructed via two-step curing process had higher fracture toughness compared to those fabricated through co-cured process. The main disadvantage of two-step curing was that the time taken was twice that required for the co-cured process. However, two-step curing is common for scarf joint applications.

Five pieces of Toray T700 CF carbon fiber plain weave fabrics were cut into sizes required for the respective testing. These five layers formed the bottom laminate layer during for the two-step curing process.

Teflon® film was first laid out on the glass surface to facilitate the removal of laminate after curing and to prevent hardening of excess resin on the surface. A layer of distribution media followed by a layer of peel ply was laid out before placing the layers of carbon fiber fabrics on top of the peel ply. The peel ply and distribution media should be about 100mm longer and 40mm wider than the size of the fabrics. Next, another layer of peel ply followed by a layer of distribution media was placed on top of the fabrics. The peel ply prevented the distribution media from adhering to the laminate during curing and yet allowed the smooth flow of the resin through the fabrics. The setup of the various layers was shown in Figure 7.

Figure 7. Arrangement of the various layers

Spiral tubing was placed at the top and bottom edge of the laminate setup to facilitate the flow of the resin. The top spiral tubing was placed on top of the top distribution media layer while the bottom tubing was placed in between the bottom distribution media and peel ply. This setup, shown in Figure 8, allowed the resin to be drawn from the bottom, through the carbon fiber layers and out through the top tube to ensure more thorough distribution. The top and bottom spiral tubing were connected to the 0.5″ solid walled polyethylene outlet (resin trap) and inlet (resin reservoir) tubing, respectively.

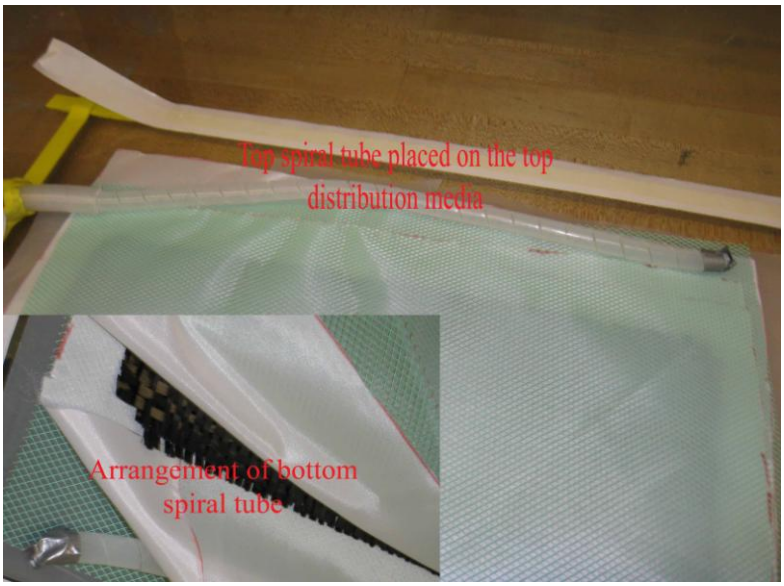

Figure 8. Arrangement of spiral tubes

The vacuum sealing around the sample was achieved using sealing tape and a vacuum bag (refer to Figure 9 and 10). A lump of sealing tape was used as a stopper to block the opening end of the inlet tube to build up the vacuum. The vacuum status was checked using the vacuum gauge connected in the setup.

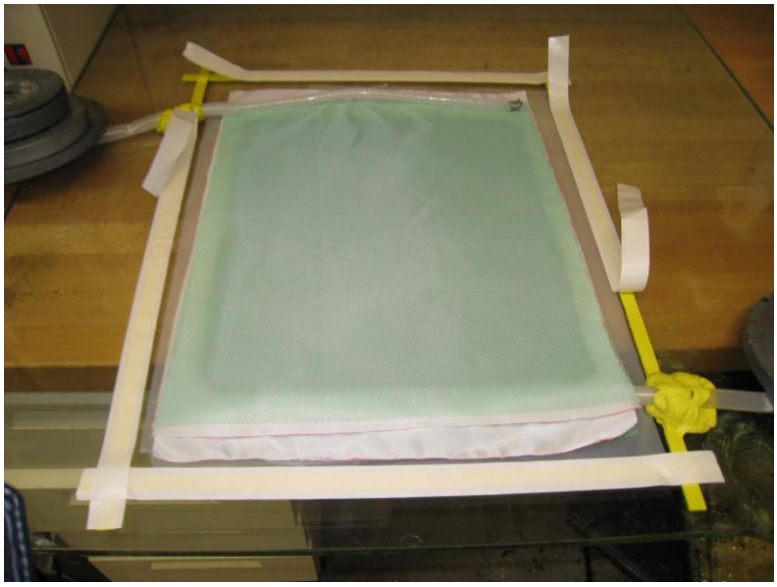

Figure 9. Sealing tape around the sample

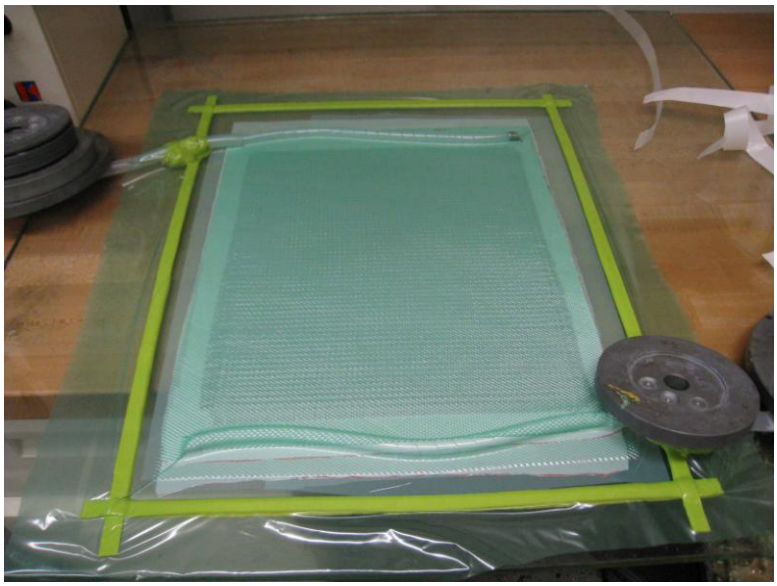

Figure 10. Vacuum achieved using vacuum bag and sealing tape

The ambient temperature was noted and the appropriate chemical concentrations, according to Table 1, were mixed with the resin in a bucket. Each chemical should be thoroughly mixed with the resin before adding the other chemical, to prevent a direct reaction between the hardening chemicals. The mixture was left to rest for about 15–20 minutes, allowing most of the air bubbles to escape as shown in Figure 11. These air bubbles, if allowed to draw through, would trap within the matrix of the sample and weakened the final product. However, the mixture should not be left to rest for too long as it might start curing. It was advised to mix in the DMA, if required, prior to drawing the resin through the fabrics.

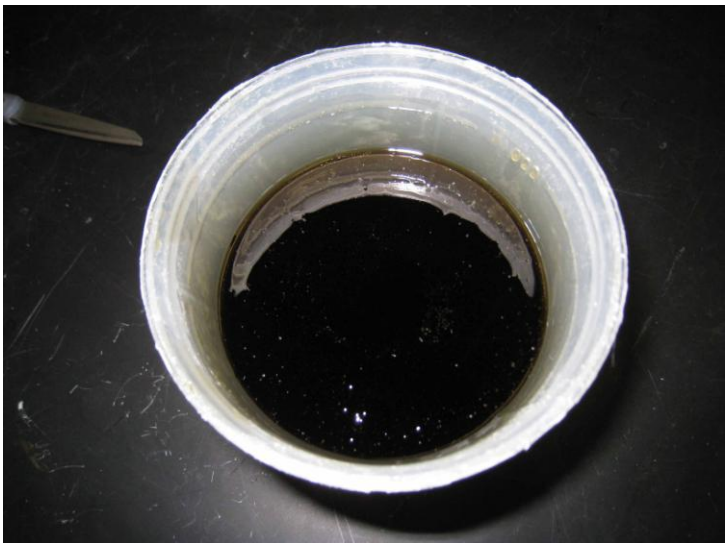

Figure 11. Resin mixture with most air bubbles dissipated

After the air bubbles dissipated, the stopper at the inlet tube was removed in the bucket to draw the resin mixture through the fabrics, as shown in Figure 12. The inlet tube was clamped to stop the flow of resin when the resin filled up to the top of the sample. The clamping also prevented any introduction of air into the sample. The resin would cure and harden within 60 minutes if the proportions of hardening chemicals were correct. The sample was left to rest for about 20 hours to ensure complete curing.

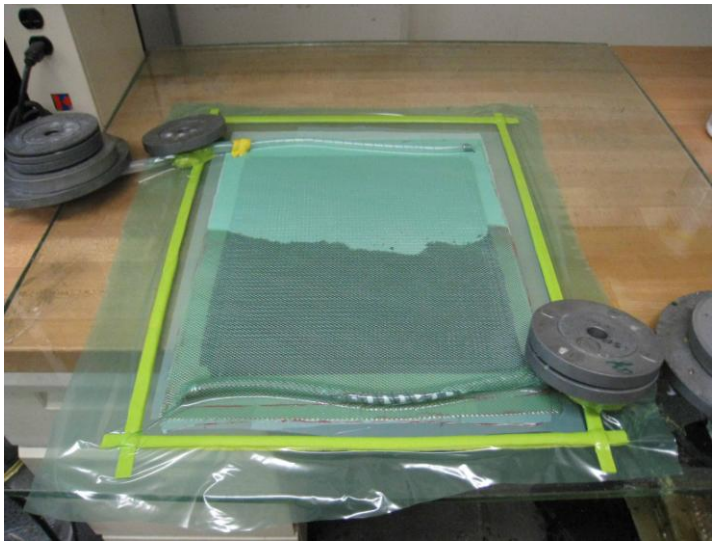

Figure 12. The VARTM process

The bottom layer of the test coupon was completed. The next step was to fabricate the complete test sample with the appropriate pre-cracked length. The surface of the bottom layer was smoothened using a 100-grit sand paper. The sanded surface was washed down with acetone to remove any loose particles. For the reinforced samples, 7.5g/m^2 CNTs or CNFs were mixed with acetone and dispersed on the cleaned surface. The acetone was allowed to dry prior to the next step. A Teflon® film, shown in Figure 13, was placed on the bottom layer to create the pre-crack. Next, another five layers of carbon fiber plain weave fabrics were laid on top and a repeat of the VARTM process produced the final sample. The samples were then cut into the required testing dimensions using a water-jet cutting machine.

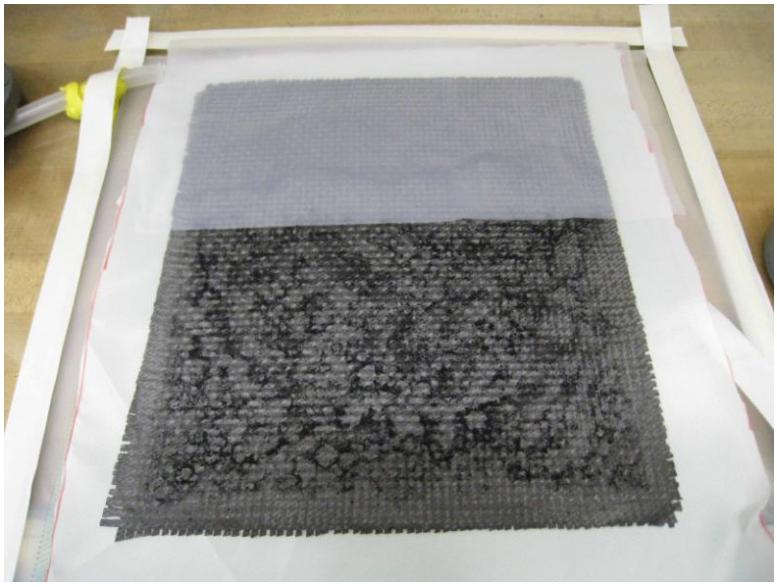

Figure 13. Dispersion of CNTs/CNFs and laying of Teflon film

THIS PAGE INTENTIONALLY LEFT BLANK

III. EXPERIMENTAL SETUP

A. CYCLIC LOADING

MTS 858 Mechanical Testing System, shown in Figure 14, was used for the cyclic testing. The samples were loaded in a 3-point bending setup at 2Hz and 10Hz cyclic frequencies. Samples were loaded at 2Hz frequency initially. Later, the frequency was increased to 10Hz to reduce the loading time for 150k cycles. No significant difference was observed between the test results at two different frequencies.

Extra precautions were needed to minimize the slippage of the specimen during the cyclic loading. The samples were first subjected to static loading on the MTS machine (at 1mm/s displacement rate) to determine the test specifications for the cyclic loading. Due to the difference in stiffness (from the results of static loading), the various samples were loaded to different displacement in order to have a comparative loading force. The non-reinforced samples were loaded to a 9mm maximum displacement and 4mm cyclic amplitude. CNTs and CNFs reinforced samples were loaded to 7mm maximum displacement and 3mm cyclic amplitude. All the samples were tested up to 150k cycles.

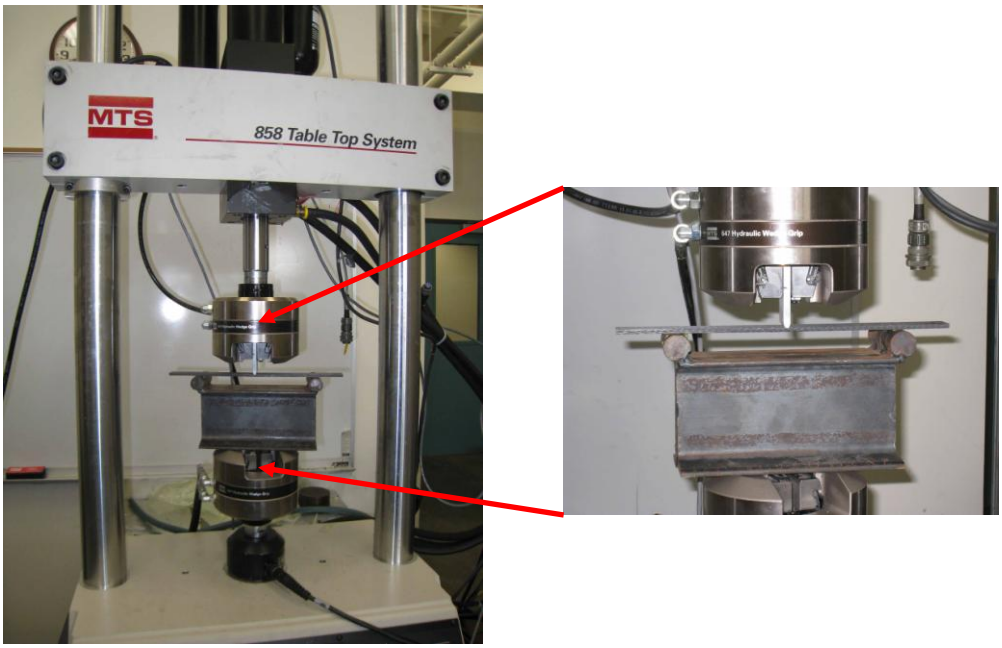

Figure 14. Static and cyclic loading on MTS 858 Mechanical Testing System

B. IMPACT TESTING

Impact testing was conducted using a specially designed drop weight instrumented testing system described in [12]. The CFRP samples were sandwiched in-between two aluminum plates at each end and clamped to the test frame, shown in Figure 15 and 16. This setup represented clamped-clamped boundary conditions and minimized slippage of samples during impact.

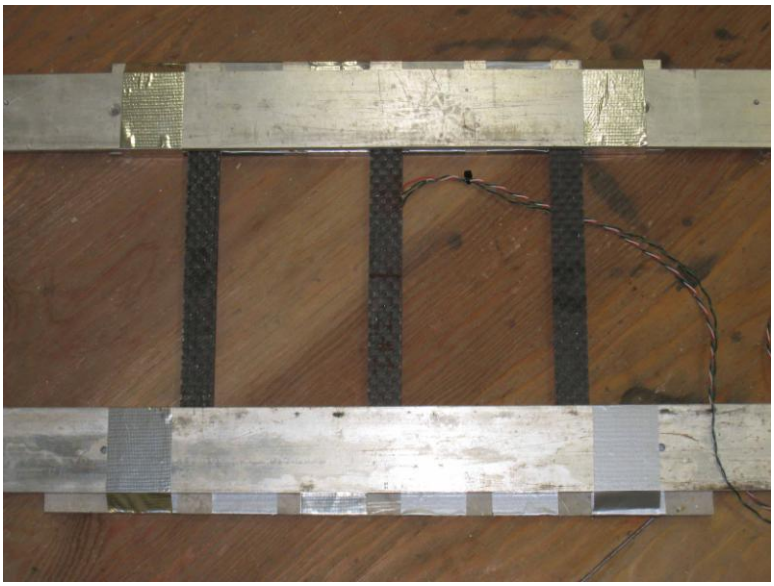

Figure 15. Securing of test sample using aluminum plates

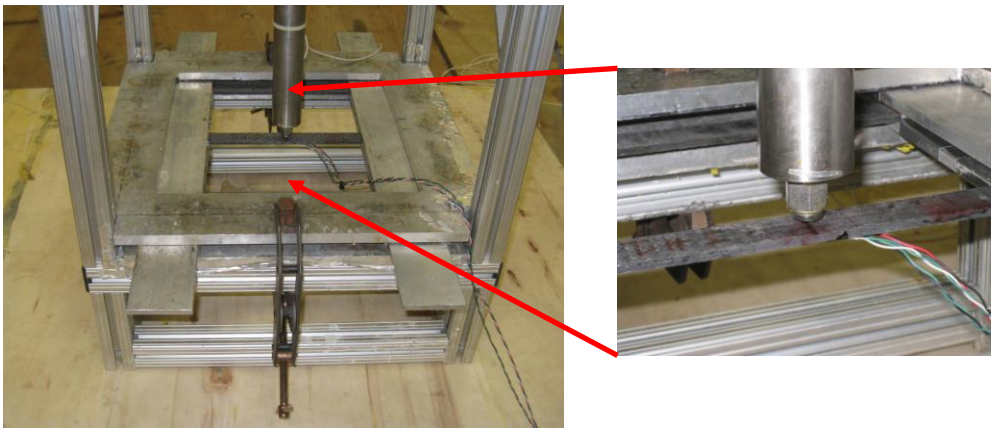

Figure 16. Clamping of test sample on impact test machine

Figure 17 showed the impact test machine lowered into the test tank to enable a more stable impact testing platform. A weight of 2kg was dropped from between 45cm to 105cm height, at a 15cm interval, to produce different impact energy. Trial tests were first conducted to determine the region where damage and crack propagation would occur.

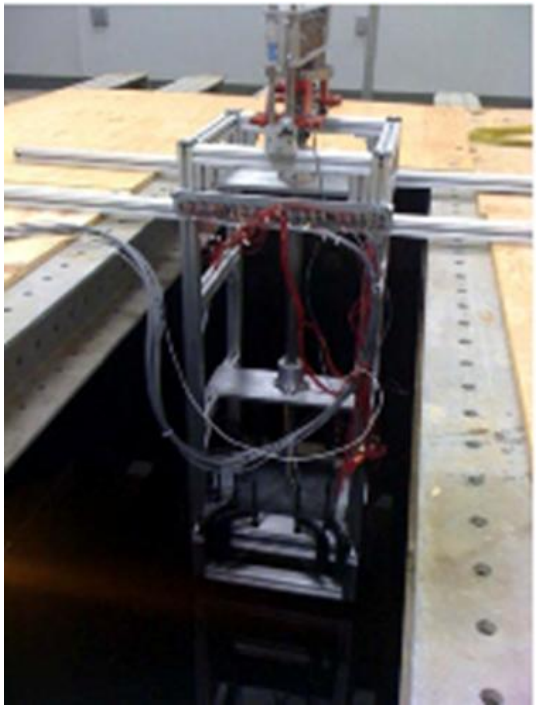

Figure 17. Impact test machine lowered into the test tank (From [13])

The transient response of the samples upon impact was measured in terms of force and strain. The force response was measured via an ICP® force sensor manufactured by PCB Piezotronics, Inc. Each sample had a strain rosette bonded at the mid-span on the underside (refer to Figure 18) for strain measurement. The strain gages used were three-element 45^{o} single plane rosettes. Only the longitudinal strain was of interest in this testing. The other two strain measurements were used to verify accuracy of data, if required.

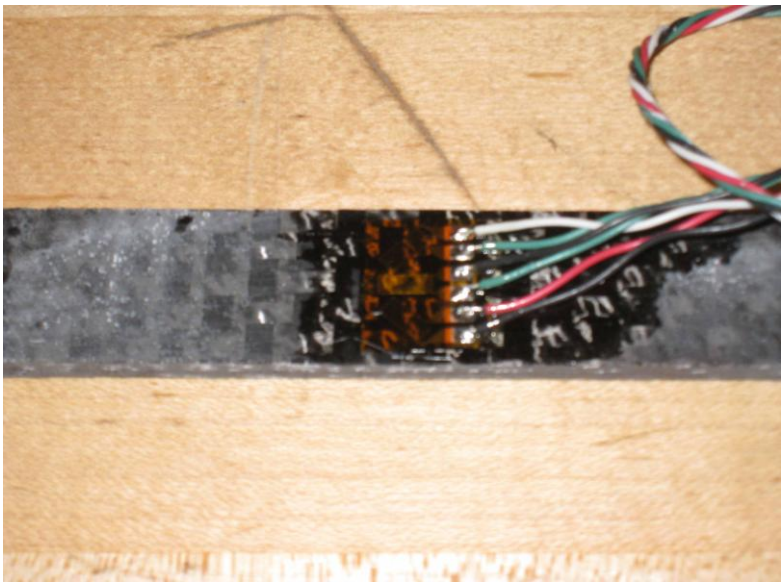

Figure 18. Strain gage bonded and on composite sample

C. OPTICAL MICROSCOPY

Crack propagation pattern of the tested samples were viewed under Nikon Epiphot 200 Inverted Metallographs. Magnification of 2.5x and 10x were observed to be the most optimum for the optical microscopy images. All the samples were examined at both surfaces of the crack propagation. This was to confirm that the crack growth was consistent across the width of the samples.

THIS PAGE INTENTIONALLY LEFT BLANK

IV. RESULTS AND DISCUSSIONS

A. STATIC LOADING

Static loading results showed that the CNTs-reinforced samples are stiffer than non-reinforced composite samples. Figure 19 showed that the majority of the crack propagations occurred at around the region of 14−16mm crosshead displacement. The displacement for cyclic testing was thus determined to be lower in the region of 7−9mm. The compressive force for the CNTs-reinforced samples was significantly higher than the non-reinforced samples, which was also observed previously in [9]. Stiffness of CNFs-reinforced samples was observed to be in-between CNTs-reinforced and non-reinforced samples. The mixed–reinforced (i.e., combined CNTs and CNFs) samples did not perform any better than the CNTs-reinforced nor CNFs-reinforced samples. Mixed-reinforced samples experienced crack propagation at compressive force of 275N, which was about 25N and 75N lower than CNFs-reinforced and CNTs-reinforced samples, respectively. Mixed-reinforced samples were discarded for subsequent testing as this type of reinforcement did not contribute any additional benefits.

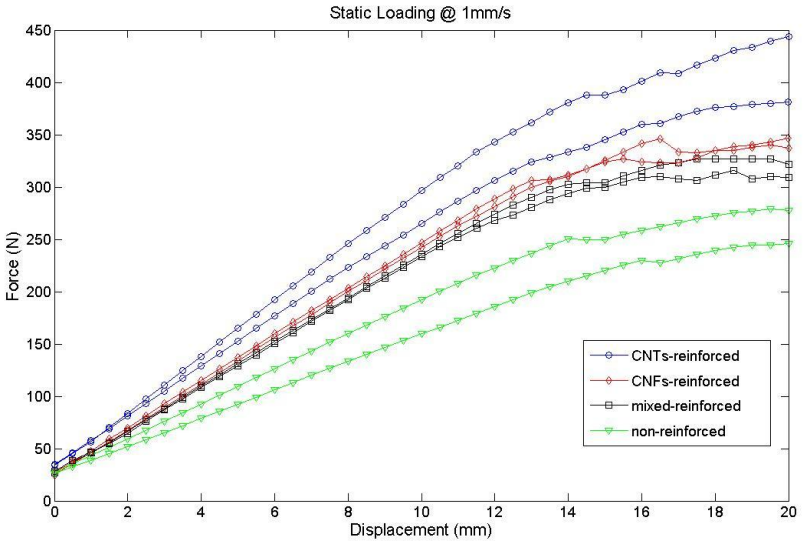

Figure 19. Load versus displacement plot for static loading

B. CYCLIC LOADING

1. Cyclic Load Data

Each sample was loaded to 150k cycles at either 2Hz or 10Hz frequencies. Each loading cycle produced a cyclic load pattern indicated in Figure 20. The F_{max} and F_{min} values were extracted from the cyclic load data and compared between the different types of samples. All graphs showed gradual decreases in the maximum and minimum forces with increasing cycles. This could be due to the accumulating micro level damage resulting in reduction of the stiffness of the samples. The initial steep change in the forces could be due to the sudden movement of the crosshead of the testing machine.

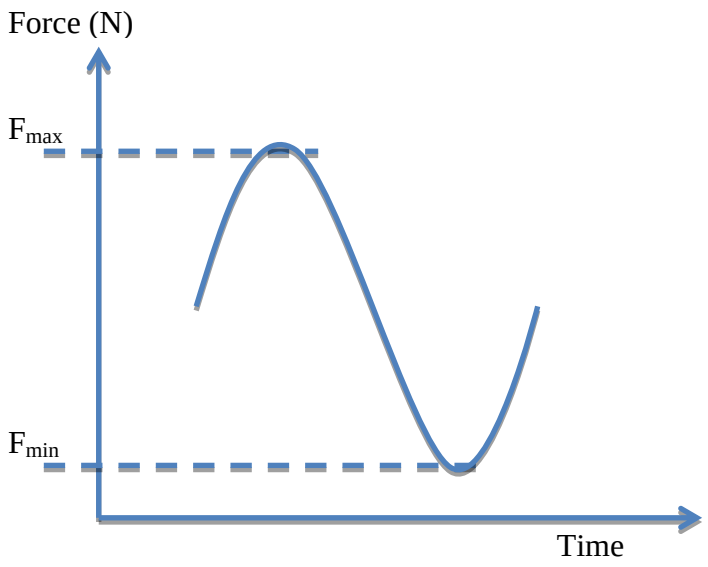

Figure 20. Example of a load cycle

The peak-to-peak (F_{max} and F_{min}) curves in Figure 21 did not vary much between CNTs-reinforced, CNFs-reinforced and non-reinforced samples. No clear-cut deduction can be derived from these data, though the reinforced samples clearly had higher load forces at the same displacement.

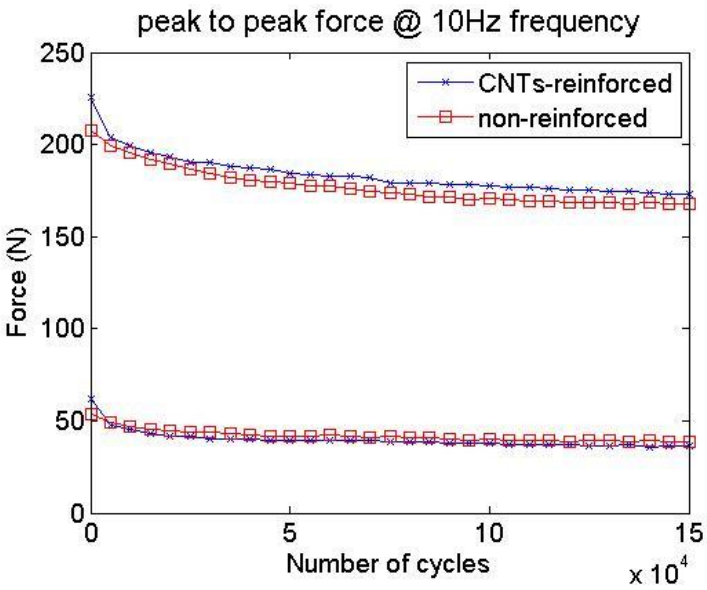

Figure 21. Peak-to-peak force (CNTs-reinforced vs. Non-reinforced)

Figure 22 showed that the comparison between loading at 10Hz and 2Hz for CNTs-reinforced samples. It was observed that there were no major differences in the load profile between samples loaded at 2Hz or 10Hz frequencies. Samples loaded at 10Hz had slightly steeper gradient in the load force, which was expected with the higher dynamic loading.

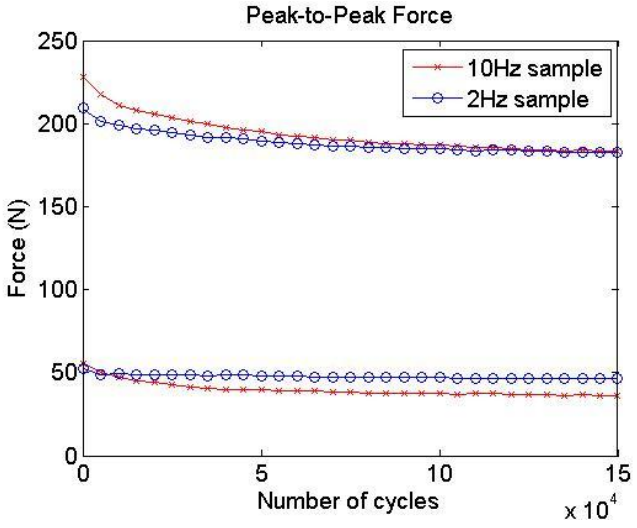

Figure 22. Peak-to-peak force for CNTs-reinforced (2Hz vs. 10Hz)

2. Crack Propagation Pattern

The crack propagation pattern was observed under microscope with 10x magnification. There were significant differences between reinforced (both CNTs and CNFs) and non-reinforced samples. Figure 23 showed a crack propagated straight through the resin matrix with little resistance inside the non-reinforced samples.

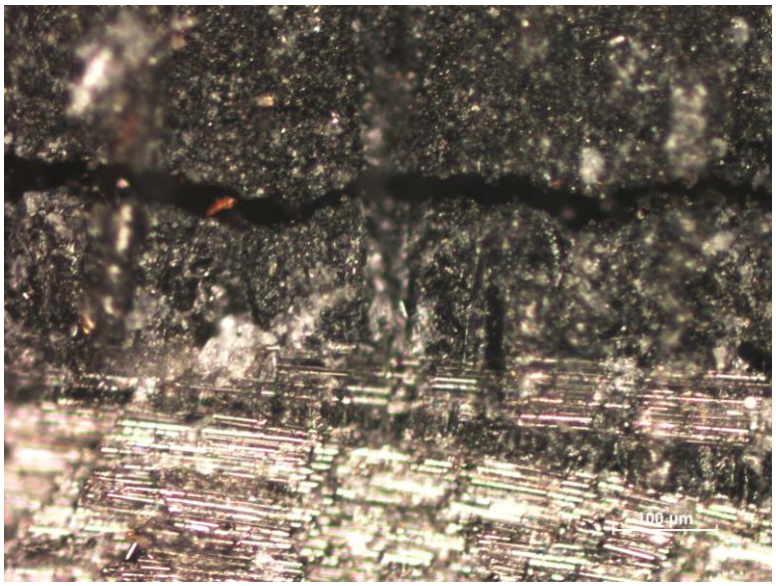

Figure 23. Crack propagation through non-reinforced sample

Very different crack propagation paths were observed in both the CNTs-reinforced and CNFs-reinforced samples. Perpendicular and 45^{o} crack propagations were widely observed in those samples (refer to Figure 24 and 25). The CNTs and CNFs reinforcement provided strong resistance to the crack propagation, making it more difficult for crack growth. This resulted in the crack propagation seeking alternative path with lower resistance, which were regions with lower or little concentration of reinforcement due to uneven dispersion of CNTs/CNFs. The stronger CNTs and CNFs bonded with the resin matrix increased the facture toughness of the joint interface. There were also evidences of crack nucleation away from the plane/path of the crack propagation but still along the joint interface. These were shown in Figure 25 and 26.

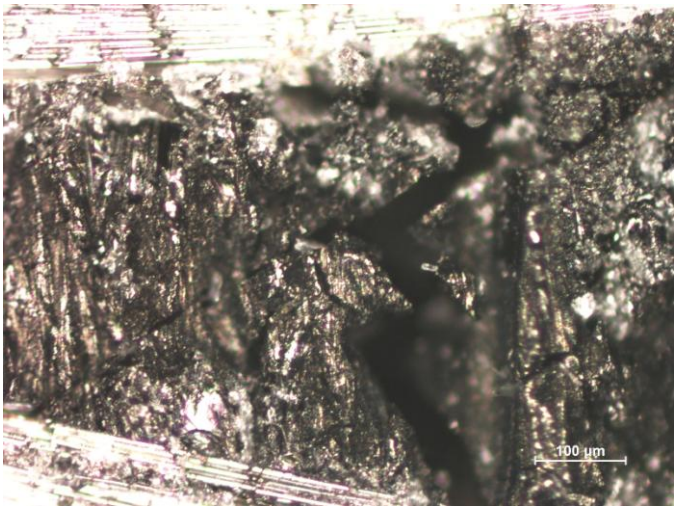

Figure 24. Perpendicular crack blocking crack propagation

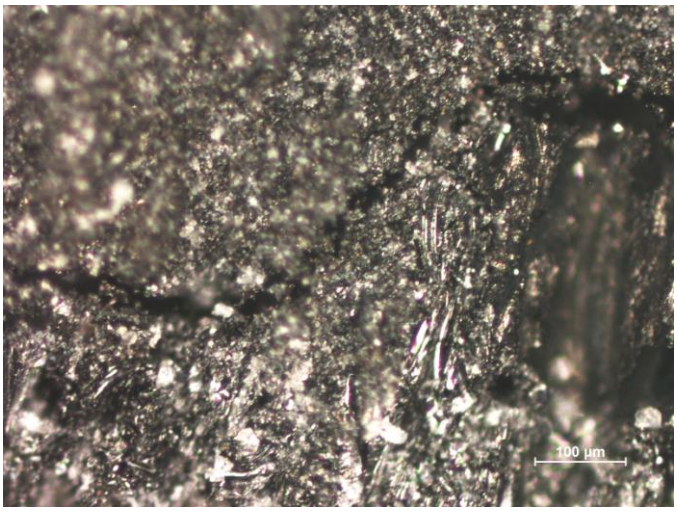

Figure 25. 45^{o} crack propagation

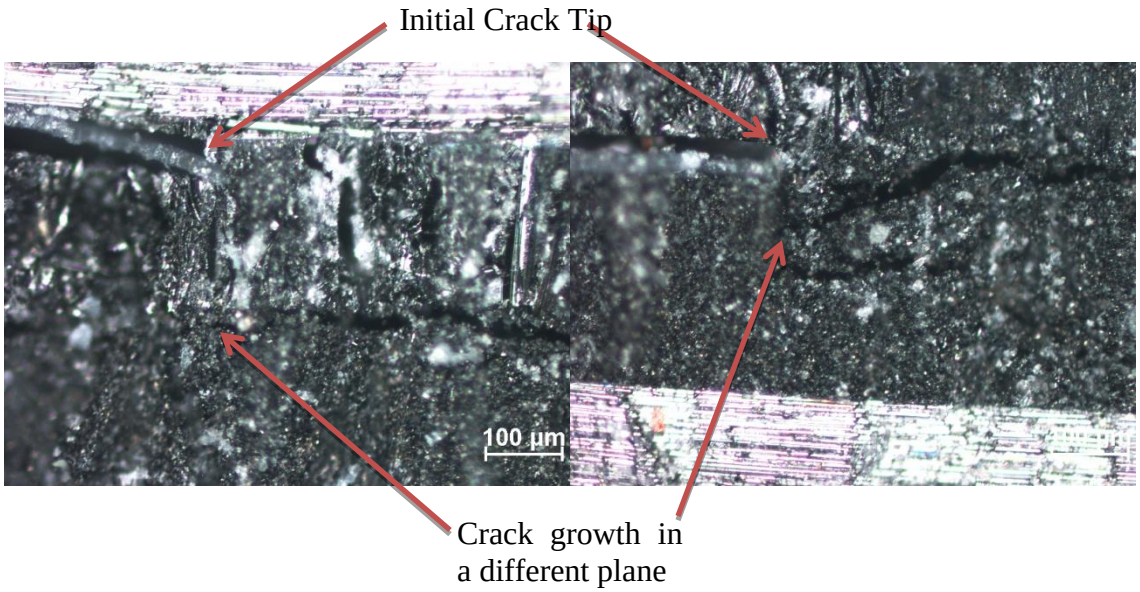

Figure 26. Crack nucleation at different plane from crack tip

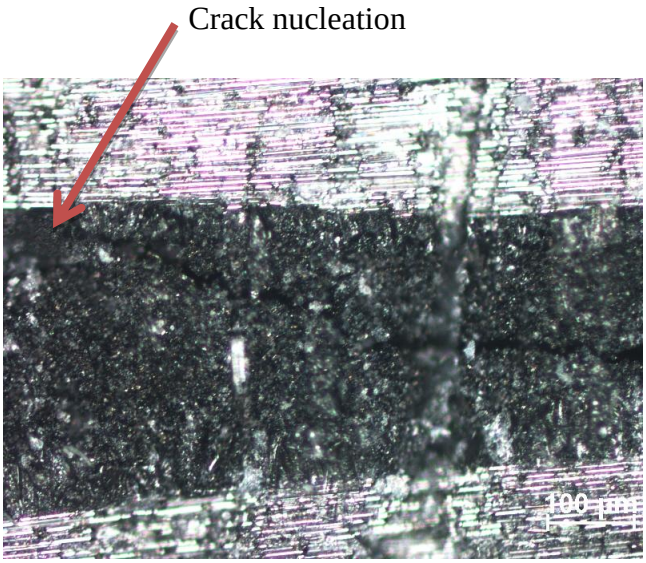

Figure 27. Crack nucleation away from crack tip along the joint interface

3. Crack Length

The crack lengths of the samples after 150k loading cycles were approximately measured by tracing the crack path under microscope. The crack lengths were averaged across all the samples as the different frequency loadings did not result in any significant difference in the crack length between the samples. The averaged crack length on the non-reinforced samples was approximately twice that of the CNTs and CNFs-reinforced samples. The shorter crack length observed on reinforced samples was mainly due to the higher resistance to crack propagation in those samples. The resistance to crack growth was previous discussed with the microscopy images. The CNTs and CNFs bonded in the resin blocked the crack propagation such that the reinforced samples would require higher loading cycles to achieve the same crack length as the non-reinforced samples. The results in Table 2 and microscopy images showed that the CNTs and CNFs reinforcement would delay crack growth and further increased structure integrity and service life.

Table 2. Averaged crack length after 150k cycles

Type	Averaged Crack Length (mm)
Non-reinforced	11.79
CNTs-reinforced	6.21
CNFs-reinforced	7.01

One of the CNTs-reinforced samples had a crack length which was relatively longer than the rest. This was due to a crack nucleated in the adjacent resin matrix away from the joint interface (refer to Figure 28). This region was not reinforced, allowing the crack to propagate through the resin matrix. Therefore, it is important to keep in consideration that any defects in the structure might cause crack nucleation away from the reinforcement region, reducing the overall fracture toughness. However, depending on the application, crack nucleation away from the joint interface might have a lesser catastrophic effect than failure at the joint interface.

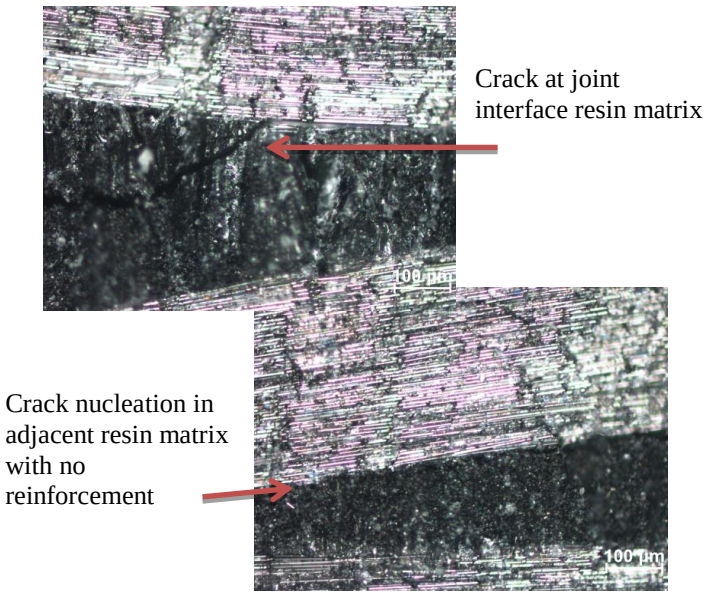

Figure 28. Nucleation of crack in adjacent resin matrix

C. IMPACT TESTING

1. Impact Force and Strain

The impact force and strain data from the impact machine for the samples were compared and analyzed. The force and strain graphs of the CNTs-reinforced samples were observed to be smoother while those for the non-reinforced samples had a more distinct "knee" shape on the recovery side (refer to Figure 29 and 30). This indicated that the non-reinforced samples suffered more damages at the respective impact height. The sudden increase in strain at 90cm drop height in Figure 29 was an indication of catastrophic failure of that particular non-reinforced sample.

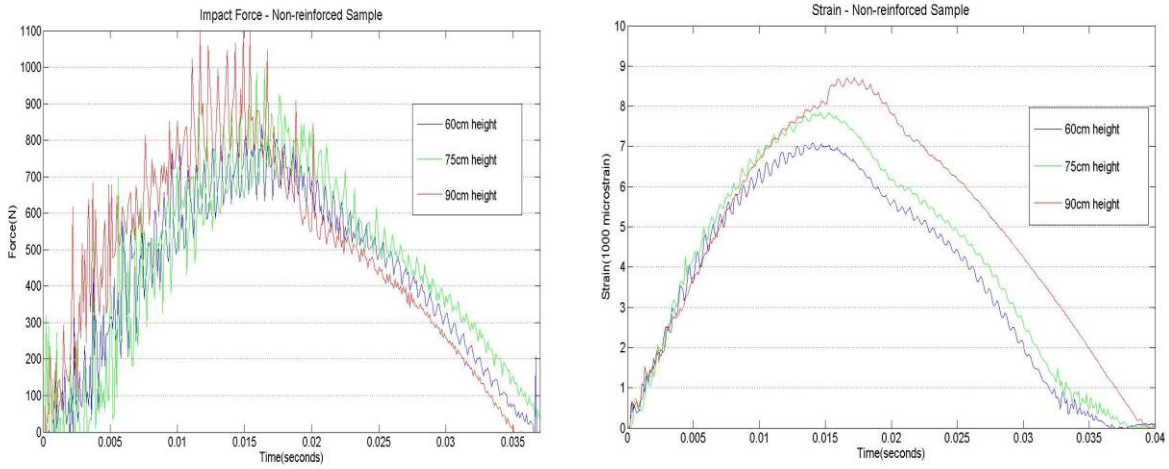

Figure 29. Impact force and strain for non-reinforced sample

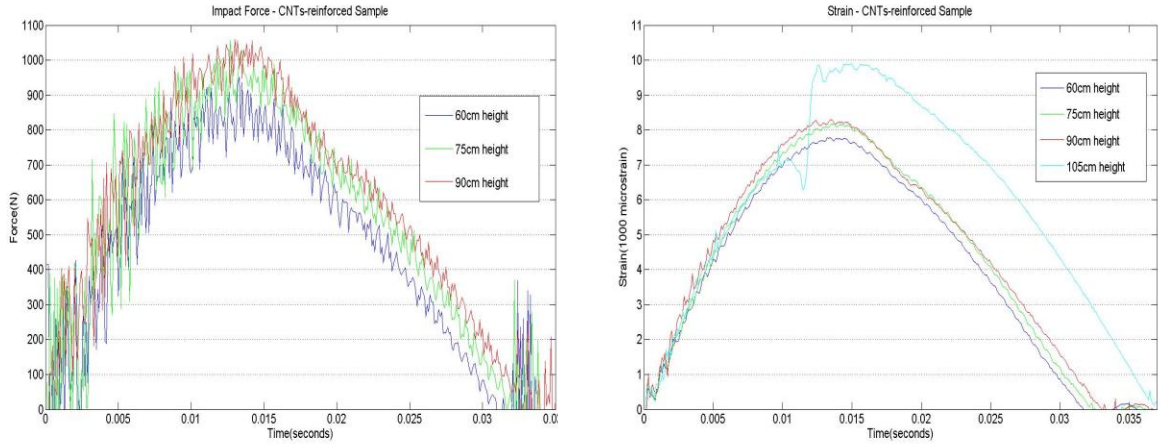

Figure 30. Impact force and strain for CNTs-reinforced sample

The plot in Figure 31 showed that the impact force for the CNTs-reinforced samples averaged about 150N higher than the non-reinforced samples. This was expected due to the increased strength and stiffness through the CNTs reinforcement at the joint interface.

The strain, however, was observed to be higher for the CNTs-reinforced samples. The difference in Figure 32 was not significant, averaging less than 500 μstrain. The CNTs reinforcement was at the neutral axis (joint interface) of the beam sample and would not significantly have increased the beam rigidity significantly. The higher impact forces experienced by the CNTs-reinforced samples therefore translated to higher strain.

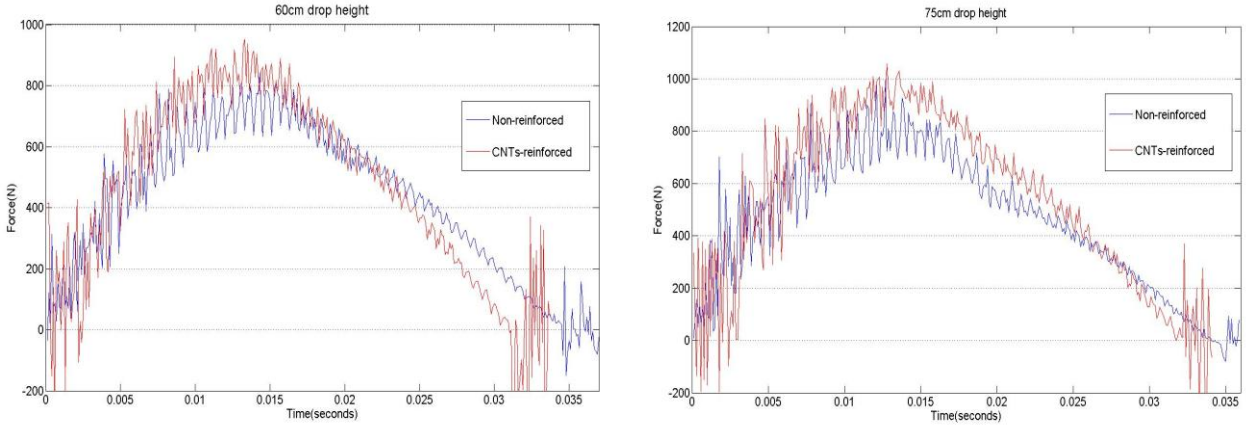

(a) (b)

Figure 31. Impact force between non-reinforced and CNTs-reinforced samples. (a) samples at 60cm drop height, (b) samples at 75cm drop height

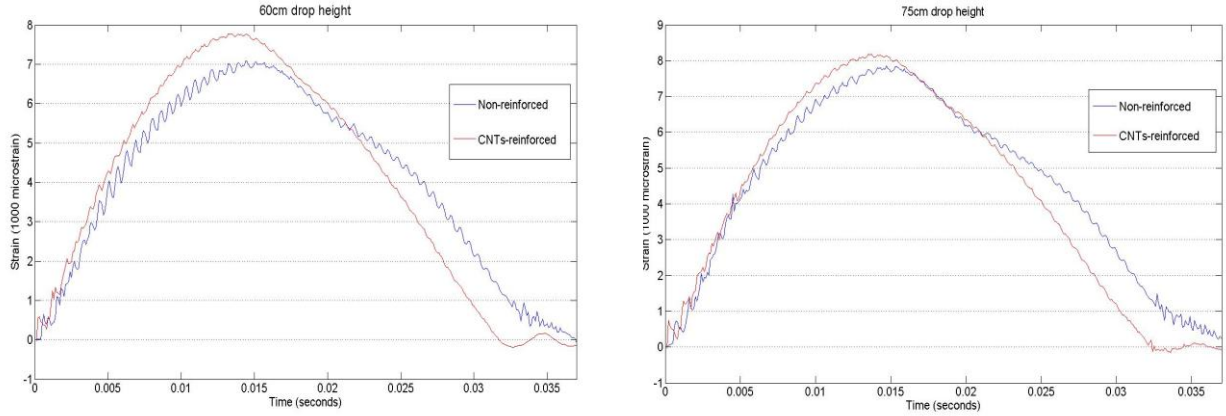

(a) (b)

Figure 32. Strain between non-reinforced and CNTs-reinforced samples. (a) samples at 60cm drop height, (b) samples at 75cm drop height

2. Crack Propagation and Crack Surface

The crack lengths for the samples were measured visually at drop heights of 75cm and 90cm and tabulated in Table 3. For the purpose of discussion in this report, failure of the sample was defined to have a crack propagated to the mid-span of the beam (crack length of 30−40mm). All the samples had comparable crack lengths at drop height of 75cm. CNFs-reinforced samples had the shortest crack length, averaging 3mm. However, the differences among the samples were not significant enough to draw a clear-cut conclusion.

Sity-six percent of the non-reinforced samples failed at subsequent drop height of 90cm, with the other 33% failing at drop height of 105cm. None of the CNTs-reinforced samples failed at 90cm drop height. The CNTs-reinforced samples failed at drop heights of 105cm and above. The stronger CNTs-reinforcement at the joint interface significantly increased the impact strength and fracture toughness of those samples.

Performance of CNFs-reinforced sample was comparable to non-reinforced sample in the impact test. 66% CNFs-reinforced samples failed at the drop height of 90cm. Increased sample size and more tests at smaller height interval might be required to have a more conclusive assessment of the influence of CNFs reinforcement under impact loading.

Table 3. Averaged crack length at drop height of 75cm and 90cm

	70cm height	**90cm height**
CNTs-reinforced	4.5mm	9.5mm (no failure at this impact height)
CNFs-reinforced	4mm	66% failure, 10mm for non-failure samples
Non-reinforced	3mm	66% failure, 12mm for non-failure samples

The samples were viewed under microscope with 2.5x magnification. The crack patterns for the non-reinforced samples were observed to be straight-through. On the CNTs-reinforced samples, multiple cracks or ‘shattered’ patterns were widely observed (refer to Figure 33). This showed that the strong CNTs bonded in the resin provided resistance to crack propagation. Higher impact force was thus required for the crack to propagate through. The crack patterns on the CNFs-reinforced samples did not differ much from that of non-reinforced samples (refer to Figure 34 and 35). The observations matched the previous discussion on the failure drop height experienced by the respective samples.

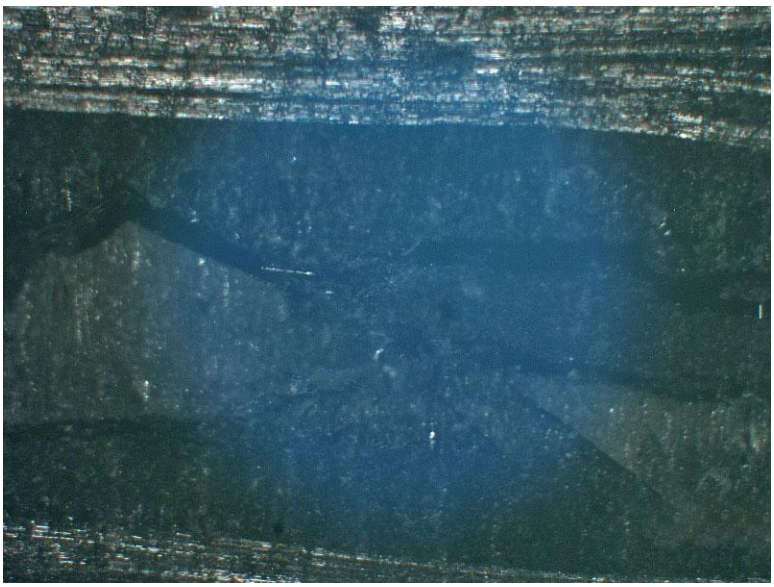

Figure 33. ‘Shattered’ crack pattern on CNTs-reinforced sample after impact test

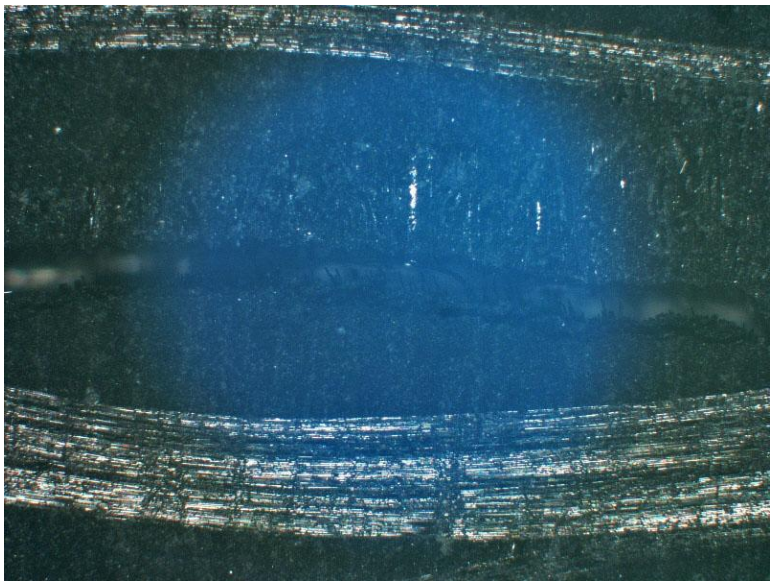

Figure 34. ‘Straight-through” crack pattern on non-reinforced sample after impact test

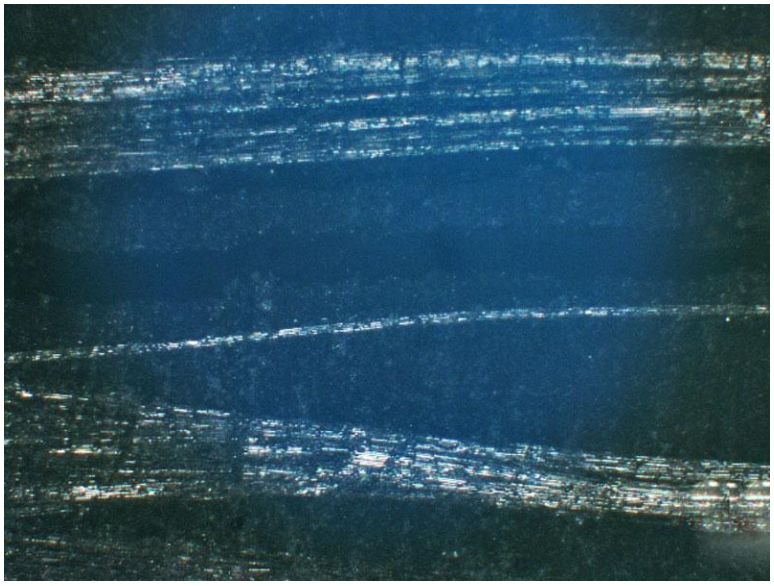

Figure 35. Crack pattern on CNFs-reinforced sample after impact test

After the testing and measurement, the samples were manually pulled apart to inspect the crack surfaces. It was observed in Figure 36 that the crack had broken through the resin on the non-reinforced samples. There were pieces of broken resin on the crack surface. Traces of the broken resin ceased at the end of the crack growth, indicating that the broken resin was due to the crack propagation during impact test.

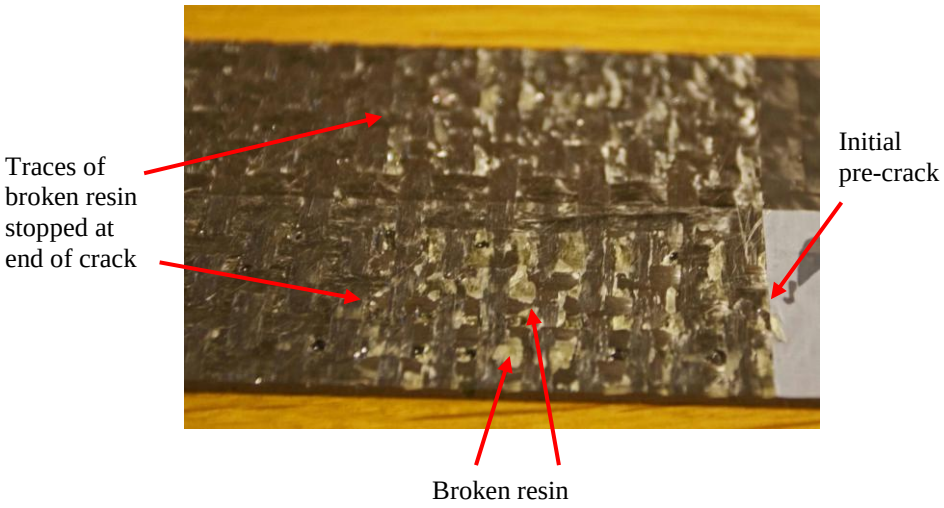

Figure 36. Crack surface of non-reinforced sample

CNTs-reinforced samples failed much differently from the non-reinforced samples. There were no obvious broken pieces of resin on the crack surface. Instead, it was observed in Figure 37 that the carbon fiber layers were broken through. This showed that the CNTs bonded to the resin at the joint interface blocked the crack propagation through the resin. The crack had to break through relatively weaker layers of carbon fiber away from the resin at joint interface. This resulted in the higher impact force required for the failure of CNTs-reinforced samples.

The breaking of the carbon fiber layers was also highlighted in Figure 38. The breakage of the carbon fiber layers resulted in a relatively more flat crack surface whereas the non-reinforced sample surface maintained the contours of intact carbon fiber fabric weave.

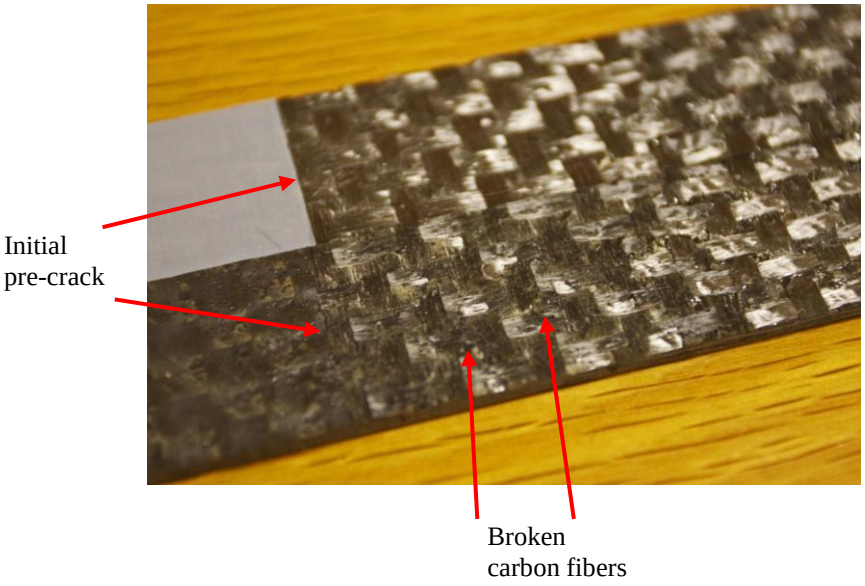

Figure 37. Crack surface of CNTs-reinforced sample

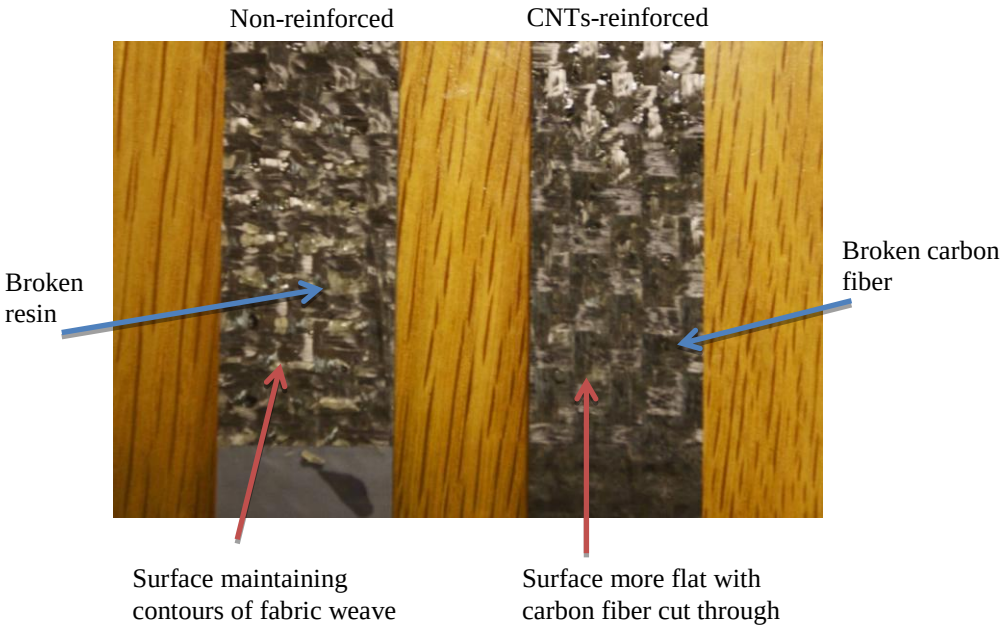

Figure 38. Comparison between crack surfaces of non-reinforced and CNTs-reinforced

THIS PAGE INTENTIONALLY LEFT BLANK

V. CONCLUSION

Many literatures had shown the positive effects of CNTs reinforcement on the strength and fracture toughness of CFRP. In particular, [5] demonstrated the improvement in properties under impact loading. The strengthening of CFRP in these researches was done via the infusion of CNTs throughout the matrix. Literatures [4] and [9]−[11] investigated on the effects of CNTs reinforcement on composite joints under static loading. Results from these literatures indicated that CNTs reinforcement improved the strength and fracture toughness of CFRP structure.

This study extended the research on CNTs reinforcement at composite joint to dynamic loading conditions, namely cyclic and impact loading. The results from this investigation further emphasized the improvement of structural properties through CNTs reinforcement. CNTs-reinforced samples displayed higher stiffness and significantly shorter crack propagation under cyclic loading. CNTs-reinforced samples also experienced failure at higher impact load compared to non-reinforced samples. The high strength CNTs bonded in the interface resin provided resistance to crack propagating through the resin. This reinforcement at the joint interface improved the overall strength and fracture toughness of the CFRP samples.

Besides CNTs reinforcement, this study also explored the possibility of using CNFs as a cheaper alternative to CNTs. CNFs reinforcement demonstrated potential in improving structural properties. CNFs-reinforced samples are stiffer than non-reinforced samples under static loading and showed higher resistance to crack propagation under cyclic loading. However, it was not conclusive for the impact testing as the results were comparable to non-reinforced samples. Further testing was recommended to establish the positive effects of CNFs reinforcement.

In conclusion, proper reinforcement of the composite joint interface using carbon nanomaterial can significantly delay the crack growth, resulting in improvement of composite structural integrity and its service life.

THIS PAGE INTENTIONALLY LEFT BLANK

APPENDIX A. CYCLIC LOADING DATA

1. Non-reinforced

	Frequency (Hz)	**Crack Length (mm)**
Sample 1	2	12.16
Sample 2	2	11.51
Sample 3	10	10.9
Sample 4	10	12.58

2. CNTs-reinforced

	Frequency (Hz)	**Crack Length (mm)**
Sample 1	2	8.26 (not used for averaged length)
Sample 2	2	5.89
Sample 3	10	6.47
Sample 4	10	6.25

3. CNFs-reinforced

	Frequency (Hz)	**Crack Length (mm)**
Sample 1	2	6.67
Sample 2	2	7.56
Sample 3	10	6.93
Sample 4	10	6.88

THIS PAGE INTENTIONALLY LEFT BLANK

APPENDIX B. IMPACT TESTING DATA

1. Non-reinforced

	Visual Crack Length (mm)	
	75cm drop height	**90cm drop height**
Sample 1	3	Failure
Sample 2	3	12
Sample 3	2	12
Sample 4	5	Failure
Sample 5	3	Failure
Sample 6	3	Failure

2. CNTs-reinforced

	Visual Crack Length (mm)	
	75cm drop height	**90cm drop height**
Sample 1	4	6
Sample 2	5	11
Sample 3	5	12
Sample 4	4	9

3. CNFs-reinforced

	Visual Crack Length (mm)	
	75cm drop height	**90cm drop height**
Sample 1	4	Failure
Sample 2	3	10
Sample 3	5	Failure

LIST OF REFERENCES

[1] R. M. Jones, *Mechanics of Composite Materials*. Philadelphia, PA: Taylor & Francis, Inc.

[2] Industrial News. (2010, February 22). *Zyvex Unveils Piranha Unmanned Surface Vehicle.* [Online]. Available http://www.compositesworld.com/news/zyvex-unveils-piranha-unmanned-surface-vehicle.

[3] Composite Technology. (2010, January 18). DDG-1000 Zumwalt: Stealth warship. [Online]. Available http://www.compositesworld.com/articles/ddg-1000-zumwalt-stealth-warship

[4] G. L. Burkholder, Y. W. Kwon, and R. D. Pollak, "Effects of carbon nanotube reinforcement on fracture strength of composite adhesive joints," *J. Material Sci.*, vol. 46, pp. 3370–3377, Dec. 2010. doi:10.1007/s10853-010-5225-6

[5] V. Kostopoulos, A. Baltopoulos, P. Karapappas, A. Vavouliotis, and A. Paipetis, "Impact and after-impact properties of carbon fiber reinforced composites enhanced with multi-wall carbon nanotubes," *Composites Sci. and Technology*, vol. 70, pp. 553–563, Nov. 2009. doi:10.1016/j.compscitech.2009.1.023

[6] A. S. Lim, Z. R. Melrose, E. T. Thostenson, and T-W. Chou, "Damage sensing of adhesively-bonded hybrid composite/steel joints using carbon nanotubes," *Composites Sci. and Technology*, vol. 71, no. 9, pp. 1183–1189, 2011.

[7] A. S. Lim, Q. An, T-W. Chou, and E. T. Thostenson, "Mechanical and electrical response of carbon nanotube-based fabric composites to Hopkinson bar loading," *Composites Sci. and Technology*, vol. 71, no. 5, pp. 616–621, 2011.

[8] L. M. Gao, E. T. Thostenson, Z. G. Zhang, and T-W. Chou, "Sensing of Damage Mechanisms in Fiber-Reinforced Composites under Cyclic Loading Using Carbon Nanotubes," *Advanced Functional Materials*, vol. 19, no. 1, pp. 123–130, 2009.

[9] S. D. Faulkner, and Y. W. Kwon, "Fracture toughness of composite joints with carbon nanotube reinforcement," *J. of Pressure Vessel Technology*, vol. 133, Apr. 2011. doi:10.1115/1.4002676

[10] Y. W. Kwon, S. Slaff, S. Barlett, and T. Greene T, "Enhancement of composite scarf joint interface strength through carbon nanotube reinforcement," *J. Material Sci.*, vol. 43, pp. 6695–6703, Apr. 2008. doi:10.1007/s10853-008-2689-8

[11] M. A. Bily, "Study of composite interface strength and crack growth monitoring using carbon nanotubes," M.S. thesis, Dept. MAE, NPS, Monterey, CA, 2009. Available http://edocs.nps.edu/npspubs/scholarly/theses/2009/Sep/09Sep%5FBily.pdf

[12] Y. W. Kwon, A. C. Owens, A. S. Kwon, and J. M. Didoszak, "Experimental study of impact on composite plates with fluid-structure interaction," *The Int. J. of Multiphysics*, vol. 4, no. 3, pp. 259–271, 2010.

[13] Y. W. Kwon, M. A. Violette, R. D. McCrillis, and J. M. Didoszak, "Transient dynamic response and failure of sandwich composite structures under impact loading with fluid structure interaction," *Appl. Composite Material,* 2012. doi: 10.1007/s10443-012-9249-8

INITIAL DISTRIBUTION LIST

1. Defense Technical Information Center
   Ft. Belvoir, Virginia

2. Dudley Knox Library
   Naval Postgraduate School
   Monterey, California

3. Young W. Kwon
   Naval Postgraduate School
   Monterey, California

4. Lt. Col. Randall D. Pollak
   AFOSR/EOARD
   London, United Kingdom

5. ME5 Meng Hwee Tan
   Republic of Singapore Navy
   Singapore

6. Rey Uncangco
   Integrated Composites Inc
   Marina, California